Materials Research. 2016; 19(6): 1319-1323
DOI: http://dx.doi.org/10.1590/1980-5373-MR-2016-0288

Titanium Dioxide Nanoparticles: Synthesis, X-Ray Line Analysis and Chemical Composition Study

Hossein Mahmoudi Chenari[a]*, Christoph Seibel[b,c], Dirk Hauschild[b,c], Friedrich Reinert[b,c], Hossein Abdollahian[d]

[a] *Department of Physics, Faculty of Science, University of Guilan, Namjoo Ave, Po Box 41335-1914, Rasht, Iran*
[b] *Experimental Physics VII and Röntgen Research Center for Complex Materials - RCCM, Universität Würzburg, Am Hubland, D-97074 Würzburg, Germany*
[c] *Karlsruhe Institute of Technology - KIT, Gemeinschaftslabor für Nanoanalytik, D-76021 Karlsruhe, Germany*
[d] *Nanotechnology Research Center of Urmia University, Urmia, Iran*

Received: April 08, 2016; Revised: July 25, 2016; Accepted: August 26, 2016

TiO_2 nanoparticleshave been synthesized by the sol-gel method using titanium alkoxide and isopropanolas a precursor. The structural properties and chemical composition of the TiO_2 nanoparticles were studied usingX-ray diffraction, scanning electron microscopy, and X-ray photoelectron spectroscopy.The X-ray powder diffraction pattern confirms that the particles are mainly composed of the anatase phase with the preferential orientation along [101] direction. The physical parameters such as strain, stress and energy density were investigated from the Williamson- Hall (W-H) plot assuming a uniform deformation model (UDM), and uniform deformation energy density model (UDEDM). The W-H analysis shows an anisotropic nature of the strain in nanopowders. The scanning electron microscopy image shows clear TiO_2 nanoparticles with particle sizes varying from 60 to 80nm. The results of mean particle size of TiO_2 nanoparticles show an inter correlation with the W-H analysis and SEM results. Our X-ray photoelectron spectroscopy spectra show that nearly a complete amount of titanium has reacted to TiO_2.

Keywords: *TiO_2;Nanoparticles;X-ray analysis;SEM;XPS*

1. Introduction

Nanometer-scale materials have recently attracted considerable scientific attention because of their beneficial high surface to volume ratio and therefore unique chemical, electronic, and physical properties. In particular TiO_2 nanoparticles are in the focus of research and thus many reports on electrical, optical, and structural properties of TiO_2 nanoparticles can be found[1-4]. B. Sathyaseelanet al.[5] investigated structural, optical and morphological properties of post-growth calcined TiO_2 nanopowder. The size dependent reflective properties of TiO_2 nanoparticles synthesizedusing arc discharge method were studied by F. Fang et al.[6] Nano-crystalline TiO_2 is a promising candidate for a wide range of applications such as photocatalysis, solar cells, dielectric materials, and photoconductors[7-10]. Modification of TiO_2 with metal and nonmetal elements has received much attention and Doped TiO_2 nanoparticles exhibit novel properties and according to impurity type, dopants improve the physical and optoelctronic paroperties of TiO_2 nanoparticles. For instance, K. Kaviyarasu et al.[11] reported the fabrication, optical and microscopic studies of magnesium doped TiO_2 NCs .optical, structural, and electronic properties of carbon-modified titanium dioxide nanoparticles synthesized by ultrasonic nebulizer spray pyrolysis have been investigated by R. Taziwa et al.[12] S. Ivanov et al.[13] studied one-step synthesis of TiO_2 nanoparticles based on the interaction between thiourea and metatitanic acid and reported the photocatalytic activity of the doped SC-TiO_2 powders. TiO_2 nanoparticles in both powder and film form can be synthesized using various methods such as chemical vapor deposition[14], chemical spray pyrolysis[15], sol-gel technique[16], hydrothermal treatment[17], and arc discharge method[18]. In this paper, the sol-gel technique has been successfully employed to synthesize TiO_2 particles on the nanometer scale.

Most of the research reports on the structural properties of nanoparticles dealt with the determination of structure type, physical and different microstructural parameters. X-ray diffraction line broadening studies give more useful information about the physical parameters such as crystallite size, dislocation density and strain.There are many analytical methods to evaluate the microstructure properties of materials such as the Scherrer's equation[19], Williamson –Hall analysis[20], the integral breadth method[21] and size strain plot method[22]. This study highlightsthe microstructure analysis and chemical composition of TiO_2 nanoparticles. Whereas only a few reports on TiO_2 nano-crystals perform X-ray photoelectron spectroscopy (XPS)[23-26].

* e-mail: mahmoudi_hossein@guilan.ac.ir and h.mahmoudiph@gmail.com

In this work, TiO_2 nanocrystals were prepared by a simple sol-gel method. A structural characterization and chemical composition study was performed by X-ray diffraction, scanning electron microscopy, and X-ray photoelectron spectroscopy. We give more information on strain-stress and the energy density of crystal by using the Williamson- Hall procedure. We also include a quantitative analysis of chemical composition of a very successful synthesized nanoparticle by surface sensitive XPS known as electron spectroscopy for chemical analysis (ESCA). The measurements suggest that nearly a complete amount of titanium has reacted to TiO_2.

2. Experimental Methods

2.1. Preparation

The preparation of TiO_2 nanoparticles was performed by the sol-gel method as follows:

The high reactivity of alkoxides in the presence of water or solutions containing isopropanol causes a formation of three-dimensional oxide networks, producing metal hydroxides (i) or hydrated oxides (ii). Hence, the general chemical reactions are given by the following equations:

$$Ti(OR)_4 + 4H_2O \rightarrow Ti(OH)_4 + 4ROH(\text{hydrolysis}), (I)$$

$$Ti(OH)_4 \rightarrow TiO_2 \times H_2O + (2-x)H_2O(\text{condensation}), (II)$$

Where R is ethyl, i-propyl, n-butyl, etc.[27]. The molar ratio of water to titanium strongly affects the stability, shape, size, and morphology of the produced alkoxide-sol. Also the size distribution of nanoparticles is dependent on the pH of solution[28]. Due to the high reactivity of titanium alkoxide ($Ti\{OCH(CH_3)_2\}_4$), 10 ml of this precursor was diluted with 40 ml of isopropanol (C_3H_7OH) at room temperature in a dry atmosphere with about 8 %relative humidity. The mixture was then added dropwise into a solution that consist of deionized water and isopropanol in a 1:1 ratio. For adjustment of the pH valuehydrochloric acid and ammonium hydroxide were added, respectively. With this addition, the acidity-alkalinity of the gel was stabilized to a pH value of 3. Subsequently, the solution was vigorously stirred for 30 minutes and a yellowish gel was formed. Afterwards, the prepared materials were washed with ethanol and the obtained gel was then dried at 120°C for two hours. A Scientific furnace(NaberthermLVD 73/23/EC) was used for calcinations of the synthesized materials at 450°C for four hours[29]. The resulting product was TiO_2 nanopowder. We will now begin to discuss the results of the structure analysis and the chemical composition measurements.

2.2. Characterization techniques

The bulk sensitive X-ray diffraction (XRD) patterns were taken with Philips X'Pertdiffractometerat room temperature using monochromatic Cu Kα (hν=8042.55 eV) excitation. Measurements were taken under beam acceleration conditions of 40 kV/35 mA. Whereas the surface sensitive X-ray photoelectron spectroscopy (XPS) measurements were performed under ultra-high vacuum (UHV) condition, in a system exhibiting a base pressure of better than 2×10^{-10} mbar. In order to study the chemical state of titanium and oxygen in the nanoparticles we used a standard non-monochromatized Mg Kα (hν = 1253.6 eV) X-ray source and a VG Clam 4 electron spectrometer. The spectra were corrected for X-ray satellites and secondary electron background (Shirley[30]) prior to analysis. Scanning electron microscopy (SEM) images of the same samples were recorded with a LED-1430VP microscope using an electron beam energy of 15 keV and a beam current of 2.62 A.

3. Results and Discussion

3.1. X-ray analysis

X-ray profile analysis is apowerfultoolin extracting the microstructure information of nanocrystallinesamples. Figure 1 shows the XRD pattern of TiO_2 nanoparticles, in the 2θ range of 10–70°.The diffraction peaks corresponding to the (1 0 1), (0 0 4), (2 0 0), (1 0 5), (2 1 1), (2 0 4) and (1 0 6) crystal planes with the lattice constants a = 3.755 Å and c = 9.5114Å confirms the anatase phases of the TiO_2 nanoparticles according to the JCPDS file 21-1272 [31]. X-ray diffraction profiles are usually influenced by crystallite size and lattice strain. According to the W-H method the individual contribution due to the size and strain can be expressed as[17]

$$B_{hkl} = B_S + \beta_D \quad (1)$$

$$B_{hkl}\cos\theta = (k\lambda/D) + 4\varepsilon\sin\theta \quad (2)$$

Where ε is the strain and D is the average crystallite size of a x-ray peak. B_{hkl} is the peak width at half-maximum intensity and B_s, β_D are the peak broadeningduetothe crystallite size and lattice strain,respectively.In the Eq. 2 the strain was assumed to be uniform in all crystallographic direction implying a uniform deformation model ('UDM'). Figure 2 (a) shows the UDM analysis.The effective crystallite size can be estimated from the extrapolation of B_{hkl} cosθ versus 4sinθ and the slop of the fitted line represents the strain.Inthe uniform deformation energy density model (UDEDM)has been replaced by ε=σ/E in equation (2); where σ is the stress of crystal and E is the modulus of elasticity in the direction perpendicular to the set of Bragg reflection. The elastic

moduli E, for the TiO_2 anatase–tetragonal assumed to be ≈174 GPa[32]. In the modified form of W-H equation called (UDEDM) model, the strain energy density u is considered and the modulus of elasticity is no longer independent. The energy density u can be determined from $u=(\varepsilon^2E)/2$ using Hooke's law. Then equation (2) can be modified again according to the energy density as

$$B_{hkl}\cos\theta = (k\lambda/D) + (4\sin\theta \times (2u/E_{hkl})^{1/2}) \quad (3)$$

In this model $B_{hkl}\cos\theta$ were plotted against $4\sin\theta / (E_{hkl}/2)^{1/2}$. The anisotropic energy density (u) from the slope of fitted line and the crystallite size calculated from the y-intercept; see Figure 2(b). The results obtained from the UDM and UDEDM models are collected in Table 1.As it is evidentfromTable1, the mean crystallite sizes obtained from the W-H models are more or less similar implying that strain in different form has very small contribution on the mean crystallite size.

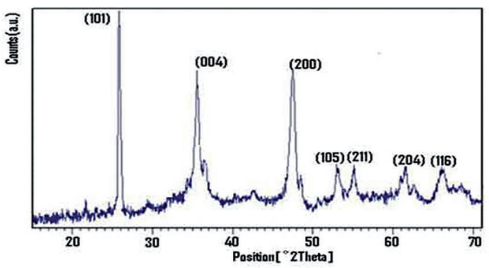

Figure 1: X-raydiffraction pattern of TiO_2 nanoparticles

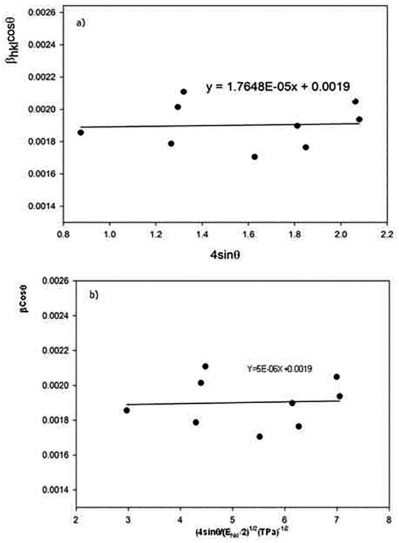

Figure 2: The W-H analysis of TiO_2 nanoparticles assuming (a) UDM, and (b) UDEDM model.

Table 1: Micro structural parameters of TiO_2 nanoparticles.

UDM model		UDEDM model			
D (nm)	ε (no unit)	D (nm)	u ($Kj.m^{-3}$)	ε (no unit)	σ (MPa)
72.2	2×10^{-5}	72.2	5.2054	5.469×10^{-6}	0.952

3.2. SEManalysis

Figure 3 shows SEM image obtained from the titanium oxide nanoparticles. The structure of this particle cluster consisting of agglomerated nanoparticles can be identified as a non-ordered and porous. In Figure 3,two particle sizes were exemplarily determined, exhibiting width of 64.82 nm (Pa 1) and 74.08 nm (Pa2). In general, the width of the nanoparticles varies from 60 to 80nm.

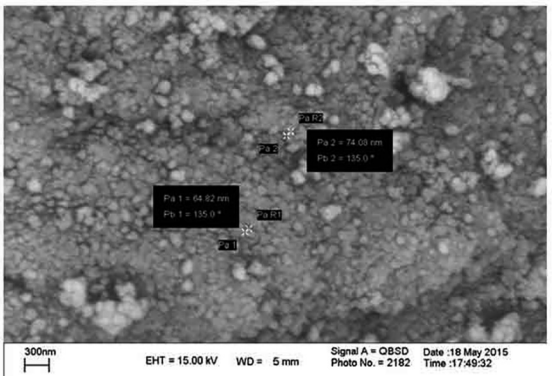

Figure 3: SEM image of theTiO_2 nanoparticles.

3.3. X-ray photoelectron spectroscopy

The powder was prepared ex-situ before transferring to the UHV chamber. Subsequent, X-ray photoelectron spectroscopy was performed and a survey scan of TiO_2 nanopowder is presented in Figure 4. To compensate charging effects, we calibrated the C1s peak to 286.0 eV since at this certain binding energy C-N and C-O bonds overlap energetically [25].The spectrum is dominated by the signals of Ti and O. The binding energies of the spin-orbit split $Ti2p_{1/2,3/2}$ (464.6 eV and 458.9 eV, respectively) signals,as well as the O 1s (530.7 eV) level are corresponding to the titanium dioxide chemical environment (see Table 2).In addition, we find a significant amount of carbon (see C 1s in Figure 4) and nitrogen (see N 1sin Figure 4) in the spectrum. The detected carbon and nitrogen contaminations stem probably from adsorbents at grain boundaries and crystallite surfaces. In general, contaminations are inevitable for samples exposed to air. However,the residual build-in contaminations resulting from the manufacturing process cannot be rule out. Furthermore, we derived the Ti:O ratio at the particle surfaces by using the corresponding cross

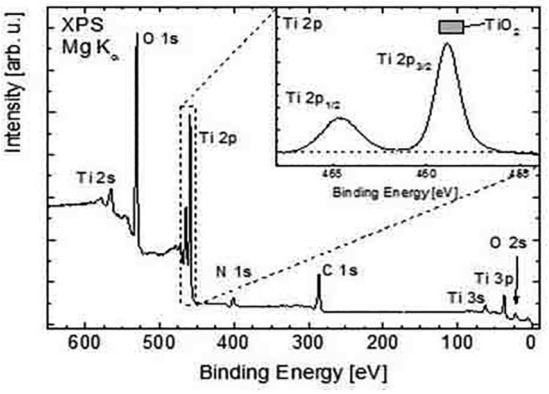

Figure 4: X-ray photoemission spectrum of TiO_2 nanoparticles taken at room temperature using a Mg X-ray source.

Table 2: Energetic positions of the Ti $2p_{1/2}$, Ti $2p_{3/2}$, and O 1s of the investigated nanoparticle sample and adsorbate. Literature values are added for comparison.

Element	Orbital	$E_{B, Exp}$ (eV)	$E_{B, Lit}$ (eV)
Titanium	$2p_{1/2}$	464.6	464.3 [34], 464.4 [35]
Titanium	$2p_{3/2}$	458.9	458.8 [34,35]
Oxygen	1s	530.7	529.6 [34], 528.4 [35]

section[26], the inelastic mean free path[33], and the transmission function $T \sim E_{kin}^{-0.6}$of our electron spectrometer. Hence, we determined a total Ti:O ratio of 1:(2.2 ± 0.4). We explain the slightly surplus of the oxygen content with adsorbents like CO_x and hydro carbons. A detailed analysis of the O1s signal reveals a small deviation from its intrinsic lineshape, which indicates several oxygen species. However, it is beyond the aim of this paper to evaluate their individual quantities and to assign them to certain contaminations.The inset of Figure 4 shows the detailed measurement of the Ti 2p region with the spin-orbit split doublet peaks at 463.9 eV and 458.2 eV for Ti $2p_{1/2}$ and Ti $2p_{3/2}$, respectively. A comparison of the obtained binding energies to the respective literature values for Ti 2p shows a good agreement between the binding energy of the main spectral 2p component and the one of pure TiO_2 (see Table 2)[34,35]. Furthermore, the absence of a signal at lower binding energies of approximately 453.8 eV[36] indicates that during the synthesis in the frame of measurement accuracy and probing depth all Ti atoms have fully reacted to titanium dioxide. The inset shows a detailed spectrum of the Ti 2p signal with a subtracted Shirley background and therefore a dashed horizontal line indicates the base line. The grey bar represents the reported Ti $2p_{3/2}$ binding energy values for TiO_2 [35].

4. Conclusions

In this study, we have successfully prepared titanium dioxide nanoparticles applying sol-gel technique. The performed X-ray diffraction measurement suggests that the precursor materials have reacted to the anatase phase .The evolution of the crystallite size and the microstrain was studied using the X-ray peak broadening analysis by the Williamson–Hall method. The obtained mean crystallite size of TiO_2 nanoparticles show an inter correlation with the value obtained from the W-H analysis and SEM results.The results of the surface sensitive X-ray photoelectron spectroscopy measurements indicate that nearly the complete amount of titanium has reacted to TiO_2.

5. Acknowledgments

The authors would like to acknowledge the Experimental Physics VII and Röntgen Research Center for Complex Materials (RCCM),UniversitätWürzburg, Am Hubland, D-97074 Würzburg, Germany and University of Guilan Research Council for the support of this work.

6. References

1. Harizanov O, Harizanova A. Development and investigation of sol–gel solutions for the formation of TiO_2 coatings. *Solar Energy Materialsand Solar Cells*. 2000;63(2):185-195.

2. Li B, Wang X, Yan M, Li L. Preparation and characterization of nano-TiO_2 powder. *Materials Chemistry and Physics*. 2002;78(1):184-188.

3. Kitiyanan A, Ngamsinlapasathian S, Pavasupree S, Yoshikawa S. The preparation and characterization of nanostructured TiO_2–ZrO_2 mixed oxide electrode for efficient dye-sensitized solar cells. *Journal of Solid State Chemistry*. 2005;178(4):1044-1048.

4. Yu C, Park J. Thermal annealing synthesis of titanium-dioxide nanowire–nanoparticle hetero-structures. *Journal of Solid State Chemistry*. 2010;183(10):2268-2273.

5. Sathyaseelan B, Manikandan E, Lakshmanan V, Baskaran I, Sivakumar K, Ladchumananandasivam R, et al. Structural, optical and morphological properties of post-growth calcined TiO_2 nanopowder for opto-electronic device application: Ex-situ studies. *Journal of Alloys and Compounds*. 2016;671:486-492.

6. Fang F, Kennedy J, Carder D, Futter J, Rubanov S. Investigations of near infrared reflective behaviour of TiO_2 nanopowders synthesized by arc discharge. *Optical Materials*. 2014;36(7):1260-1265.

7. Santangelo S, Messina G, Faggio G, Donato A, De Luca L, Donato N, et al. Micro-Ramananalysis of titanium oxide/carbonnanotubes-based nanocomposites for hydrogen sensing applications. *Journal of Solid State Chemistry*. 2010;183(10):2451-2455.

8. Morris D, Egdell RG. Application of V-doped TiO_2 as a sensor for detection of SO_2. *Journal of Materials Chemistry*. 2001;11:3207-3210.

9. Xu X, Zhao J, Jiang D, Kong J, Liu B, Deng J. TiO_2 sol-gel derived amperometric biosensor for H_2O_2 on the electropolymerized phenazine methosulfate modified electrode. *Analytical and Bioanalytical Chemistry*. 2002;374(7):1261-1266.

10. Ding Z, Hu X, Lu GQ, Yue PL, Greenfield PF. Novel Silica Gel Supported TiO_2 Photocatalyst Synthesized by CVD Method. *Langmuir*. 2000;16(15):6216-6222.

11. Kaviyarasu K, Premanand D, Kennedy J, Manikandan E. Synthesis of mg doped TiO_2 nanocrystals prepared by wet-chemical method: optical and microscopic studies. *International Journal of Nanoscience*.2013;12(5):1350033.

12. Taziw R, Meyer EL, Sideras-Haddad E, Erasmus RM, Manikandan E, Mwakikunga BW. Effect of Carbon Modification on the Electrical, Structural, and Optical Properties of TiO_2 Electrodes and Their Performance in Labscale Dye-Sensitized Solar Cells. *International Journal of Photoenergy*. 2012;2012:904323.

13. Ivanov S, Barylyak A,Besaha K, Bund A, Bobitski Y, Wojnarowska-Nowak R, et al. Synthesis, Characterization, and Photocatalytic Properties of Sulfur- and Carbon-Codoped TiO_2 Nanoparticles. *Nanoscale Research Letters*. 2016;11:140.

14. Wang Y, HaoY, Cheng H, Ma J, Xu B, Li W, et al.The photoelectrochemistry of transition metal-ion-doped TiO_2 nanocrystalline electrodes and higher solar cell conversion efficiency based on Zn2+-doped TiO_2 electrode. *Journal of Materials Science*. 1999;34(12):2773-2779.

15. Li X, Chen G, Po-Lock Y, Kutal C. Photocatalytic oxidation of cyclohexane over TiO_2 nanoparticles by molecular oxygen under mild conditions. *Journal of Chemical Technology and Biotechnology*. 2003;78(12):1246-1251.

16. Hemissi M, Amardjia-Adnani H.Optical and Structural properties of titanium oxide thin films prepared by sol-gel methods. *Digest Journal of Nanomaterials and Biostructures.* 2007;2(4):299-305.

17. Reddy KM, Manurama SV, Reddy AR. Bandgap studies on anatase titanium dioxide nanoparticles. *Materials Chemistry and Physics*. 2002;78(1):239-245.

18. Fang F, Kennedy J, Manikandan E, Futter J, Markwitz A. Morphology and characterization of TiO_2 nanoparticles synthesized by arc discharge. *Chemical Physics Letters*. 2012;521:86-90.

19. Scherrer P. Bestimmung der Größe und der inneren Struktur von Kolloidteilchen mittels Röntgenstrahlen. *Nachrichten von der Gesellschaft der Wissenschaften zu Göttingen, Mathematisch-Physikalische Klasse*. 1918;1918:98-100.

20. Williamson GK, Hall WH. X-ray line broadening from filed aluminium and wolfram. *Acta Metallurgica*. 1953;1(1):22-31.

21. Santra K, Chatterjee P, Sen Gupta SP. Voigt modelling of size-strain analysis: Application to α-Al_2O_3 prepared by combustion technique. *Bulletin of Materials Science*. 2002;25(3):251-257.

22. Prabhu YT, Venkateswara Rao K, Sesha Sai Kumar V, Siva Kumari B. X-ray Analysis of Fe doped ZnO Nanoparticles by Williamson-Hall and Size-Strain Plot. *International Journal of Engineering and Advanced Technology*. 2013;2(4):268-274.

23. Madhu Kumar P, Badrinarayanan S, Sastry M. Nanocrystalline TiO_2 studied by optical, FTIR and X-ray photoelectron spectroscopy: correlation to presence of surface states. *Thin Solid Films*. 2000;358(1-2):122-130.

24. Vorkapic D, Matsoukas T. Effect of Temperature and Alcohols in the Preparation of Titania Nanoparticles from Alkoxides. *Journal of the American Ceramic Society*. 1998;81(11):2815-2820.

25. Yeh JJ, Lindau I.Atomic subshell photoionization cross sections and asymmetry parameters: $1 \leq Z \leq 103$. *Atomic Data and Nuclear Data Tables*.1985;32(1):1-155.

26. Tanuma S, Powell CJ, Penn DR. Calculations of electron inelastic mean free paths. V. Data for 14 organic compounds over the 50–2000 eV range. *Surface and Interface Analysis*. 1994;21(3):165-176.

27. Karami A. Synthesis of TiO_2 nano powderby the sol-gel method and its use as a photocatalyst. *Journal of the Iranian Chemical Society*. 2010;7(2 Suppl):S154-S160.

28. Look JL, Zukoski CF. Colloidal Stability and Titania Precipitate Morphology: Influence of Short-Range Repulsions. *Journal of the American Ceramic Society*. 1995;78(1):21-32.

29. Nagpal VJ, Davis RM, Riffle JS. In situ steric stabilization of titanium dioxide particles synthesized by a sol-gel process. *Colloids and Surfaces A: Physicochemical and Engineering Aspects*.1994;87(1):25-31.

30. Shirley DA. High-Resolution X-Ray Photoemission Spectrum of the Valence Bands of Gold.*Physical Review B*. 1972;5(12):4709-4713.

31. Arami H, Mazloumi M, Khalifehzadeh R, Sadrnezhaad SK. Sonochemical preparation of TiO_2nanoparticles. *Materials Letters*. 2007;61(23-24):4559-4561.

32. Borgese L, Bontempi E, Gelfi M, Depero LE, Goudeau P, Geandier G, et al. Microstructure and elasticproperties of atomiclayerdeposited TiO_2 anatasethin films. *Acta Materialia*. 2011;59(7):2891-2900.

33. Shu-Xin W, Zhi M, Yong-Ning Q, Fei H, Li Shan J, Yan-Jun Z. XPS study of Cooper dopping TiO_2 photocatalyst. *Acta Physico-Chimica Sinica*. 2003;19(10):967-969.

34. Fang J,Bi X, Si D, Jiang Z, Huang W. Spectroscopic studies of interfacial structures of CeO_2–TiO_2mixed oxides. *Applied Surface Science*. 2007;253:8952-61.

35. Naumkin AV, Kraut-Vass A, Gaarenstroom SW, Powell CJ. *NIST X-Ray Photoelectron Spectroscopy Database 20,Version 4.1*. Washington: U.S. Secretary of Commerce; 2012.

36. Moulder JF, Stickle WF, Sobol PE, Bomben KD. *Handbook of X-ray photoelectron spectroscopy: a reference book of standard spectra for identification and interpretation of XPS data*. Eden Prairie: Physical Electronics Division,Perkin-Elmer Corp; 1992. 261 p.